UC Santa Cruz
UC Santa Cruz Previously Published Works

Title

Yersinia pseudotuberculosis YopD mutants that genetically separate effector protein translocation from host membrane disruption

Permalink

https://escholarship.org/uc/item/8q61b7vr

Journal

Molecular Microbiology, 96(4)

ISSN

0950-382X

Authors

Adams, Walter
Morgan, Jessica
Kwuan, Laura
et al.

Publication Date

2015-05-01

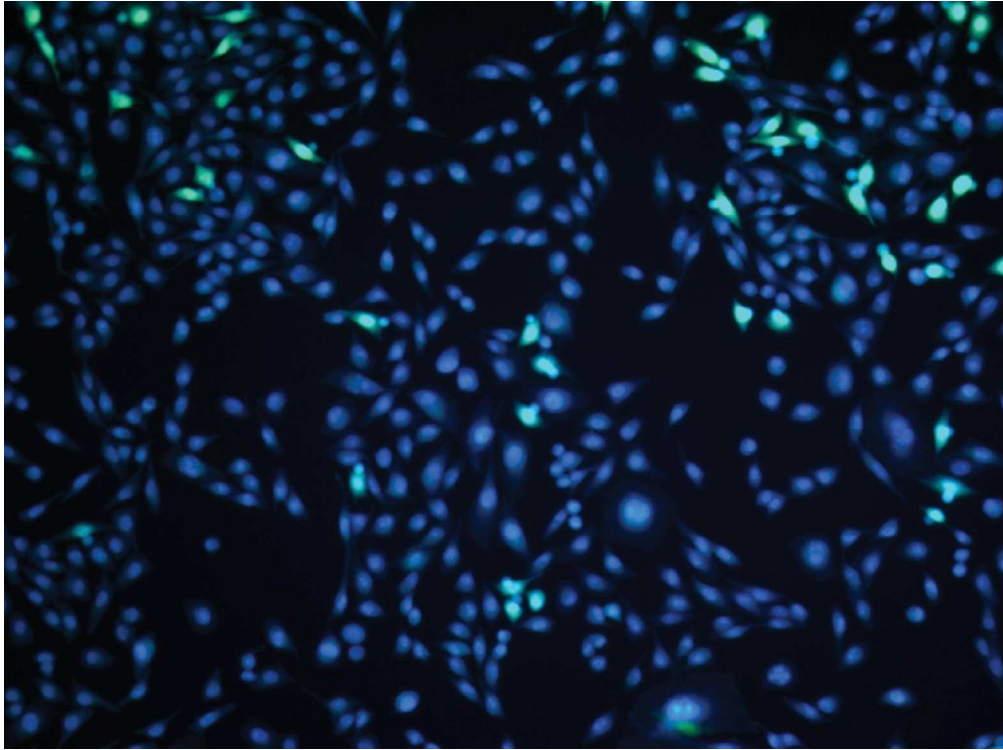**DOI**

10.1111/mmi.12970

Copyright Information

Peer reviewed

Yersinia pseudotuberculosis YopD mutants that genetically separate effector protein translocation from host membrane disruption.

SCHOLARONE™
Manuscripts

Abbreviated Abstract

YopD plays a critical role in the ability of the *Yersinia* type III secretion system to inject effector proteins into target host cells. Here we characterize the central region of YopD and show that it is important for robust translocation of multiple effector proteins into host cells such as macrophages and neutrophils. Without the YopD central region, *Yersinia pseudotuberculosis* is defective in effector protein-mediated inhibition of host defenses and is attenuated for virulence.

80x59mm (300 x 300 DPI)

1

Yersinia pseudotuberculosis YopD mutants that genetically separate effector protein translocation from host membrane disruption.

4

Walter Adams[1][*], Jessica Morgan[2], Laura Kwuan[1][**], and Victoria Auerbuch[1][***]

7

Keywords: T3SS, YopD, *Yersinia*, respiratory burst, macrophage, neutrophil.

Running Title: YopD central region promotes Yop translocation.

10

[1] Department of Microbiology and Environmental Toxicology, [2] Department of Chemistry and Biochemistry, University of California Santa Cruz, Santa Cruz, CA, USA

[*]Current address: Department of Molecular Biology and Microbiology, Tufts University School of Medicine.

[**]Current address: Quality Control Microbiology, Genentech Inc., South San Francisco, CA, USA.

[***]Corresponding author.
1156 High Street Santa Cruz, CA 95064
831-459-3049 (phone)
831-459-3524 (fax)
vastone@ucsc.edu

26

27

1

28   **Summary**

29   The *Yersinia* type III secretion system (T3SS) translocates Yop effector proteins into

30   host cells to manipulate immune defenses such as phagocytosis and reactive oxygen

31   species (ROS) production. The T3SS translocator proteins YopB and YopD form pores

32   in host membranes, facilitating Yop translocation. While the YopD amino and carboxy

33   termini participate in pore formation, the role of the YopD central region between amino

34   acids 150-227 remains unknown. We assessed the contribution of this region by

35   generating *Y. pseudotuberculosis* $yopD_{\Delta150-170}$ and $yopD_{\Delta207-227}$ mutants and analyzing

36   their T3SS functions. These strains exhibited wildtype levels of Yop secretion *in vitro*

37   and enabled robust pore formation in macrophages. However, the $yopD_{\Delta150-170}$ and

38   $yopD_{\Delta207-227}$ mutants were defective in Yop translocation into CHO cells and splenocyte-

39   derived neutrophils and macrophages. These data suggest that YopD-mediated host

40   membrane disruption and effector Yop translocation are genetically separable activities

41   requiring distinct protein domains. Importantly, the $yopD_{\Delta150-170}$ and $yopD_{\Delta207-227}$ mutants

42   were defective in Yop-mediated inhibition of macrophage cell death and ROS

43   production in neutrophil-like cells, and were attenuated in disseminated *Yersinia*

44   infection. Therefore, the ability of the YopD central region to facilitate optimal effector

45   protein delivery into phagocytes, and therefore robust effector Yop function, is important

46   for *Yersinia* virulence.

47

48

49

50

2

Introduction

Dozens of Gram negative pathogens use a type III secretion system (T3SS) to inject

bacterial effector proteins inside eukaryotic host cells. This includes all three species of

Yersinia that are pathogenic to humans: *Yersinia pestis,* the causative agent of bubonic

plague, as well as the two enteropathogens *Yersinia enterocolitica* and *Yersinia*

pseudotuberculosis. While enteropathogenic *Yersinia* infections are usually self-limiting

in healthy individuals, mortality rates approach 50% in immunocompromised patients

(Cover and Aber, 1989). The Ysc T3SS is highly conserved in *Yersinia* and is

comprised of approximately 25 structural proteins and a translocon complex made up of

three translocator proteins: YopB, YopD, and LcrV (Cornelis, 2006; Diepold *et al.*,

2010). Importantly, these three components are all essential for pore formation in host

cell membranes, enabling entry of six effector proteins (YopHOTJEM) into the host

cytosol (Rosqvist *et al.*, 1994; Pettersson *et al.*, 1996; Neyt and Cornelis, 1999;

Cornelis, 2006). Once inside the host cytosol, these effector proteins disrupt a number

of host processes, such as phagocytosis, inflammatory cytokine and reactive oxygen

species (ROS) production, and cell death pathways, promoting *Yersinia* virulence

(Viboud and Bliska, 2005; Philip and Brodsky, 2012).

Both neutrophils and macrophages use an NADPH oxidase complex to produce

superoxide anions in response to inflammatory stimuli (Takeya and Sumimoto, 2003;

Segal, 2005; Keith *et al.*, 2009). Ultimately, this process generates a diverse set of

bactericidal ROS important in the host response to invading pathogens. To counter this

host response, *Yersinia* inhibit ROS production through the action of two different T3SS

3

74   effector proteins, YopH and YopE. YopH is a tyrosine phosphatase that inhibits the Fc

75   receptor-mediated respiratory burst in both neutrophils and macrophages (Bliska and

76   Black, 1995; Ruckdeschel *et al.*, 1996). YopE uses its GTPase activating protein

77   (RhoGAP) activity to inhibit the essential NADPH oxidase component Rac2, dampening

78   ROS production in neutrophils and macrophages (Ruckdeschel *et al.*, 1996;

79   Songsungthong *et al.*, 2010). Importantly, *Y. pseudotuberculosis* YopE mutants with a

80   specific defect in targeting Rac2 are attenuated in a mouse infection model, suggesting

81   YopE-mediated inhibition of ROS production is important for virulence (Songsungthong

82   *et al.*, 2010).

83

84   Programmed host cell death is one important outcome of the immune response to

85   pathogenic microbes. Three different *Yersinia* effector Yops, YopJ, YopM, and YopE,

86   have been shown to manipulate host cell survival and death pathways in distinct ways.

87   YopJ inhibits the host NFκB and MAP kinase pro-survival pathways and may activate

88   the cell death protease caspase-1 (Philip and Brodsky, 2012). YopM directly binds to

89   and inhibits the activity of caspase-1 (LaRock and Cookson 2012). In addition, Rac1

90   targeting by YopE has been shown to inhibit caspase-1 activity (Schotte *et al.*, 2004).

91   The overall outcome of host cell death and survival as a result of these effector Yops

92   depends upon the *Yersinia* genetic background, host cell type, and host cell activation

93   state (Bergsbaken *et al.*, 2009).

94

95   YopB and YopD are thought to form the conduit in the host cell membrane through

96   which T3SS cargo enters host cells. However, the structure of this conduit remains

97   unclear (Montagner *et al.*, 2011). YopB contains two transmembrane domains, one of

98   which has been shown to be essential for host membrane pore formation (Ryndak *et al.*,

99   2005). YopD contains one putative transmembrane domain between amino acids 128

100   and 149 that increases the robustness of host membrane disruption as well as pore size

101   (Olsson *et al.*, 2004; Kwuan *et al.*, 2013). However, YopD also contains a central region

102   between amino acids 150-227 that was previously shown to be completely dispensable

103   for pore formation on red blood cells (Olsson *et al.*, 2004). Deletion of YopD amino

104   acids 171-206 was shown to be associated with enhanced effector protein translocation,

105   while deletion of YopD amino acids 150-170 or 207-227 did not lead to any detectable

106   phenotype in a variety of *in vitro* and cell culture infection assays (Olsson *et al.*, 2004).

107   Yet the YopD$_{150-170}$ and YopD$_{207-227}$ regions share 100% amino acid identity with YopD

108   from *Y. enterocolitica* and *Y. pestis*, indicating that the YopD region may play a specific

109   role in *Yersinia* fitness.

110

111   In this study, we investigated the role of the YopD central region in type three secretion

112   and *Yersinia* virulence by generating *Y. pseudotuberculosis* mutants carrying in-frame

113   deletions of YopD amino acids 150-170 or 207-227. Our results indicate that these

114   regions of YopD are dispensable for YopBD-mediated pore formation in macrophages,

115   yet play a role in efficient translocation of T3SS effector proteins into host cells. This

116   Yop translocation defect is correlated with decreased effector Yop activity, such as

117   inhibition of phagocyte ROS production and cell death pathway manipulation, and a

118   subsequent dampening of *Yersinia* virulence. These findings suggest that, in addition to

119   disrupting the host membrane to allow passage of T3SS cargo, YopD facilitates optimal

120 effector protein entry into host cells to maintain sufficient Yop activity and promote full

121 virulence.

122

123

124 **<u>Results</u>**

125 *Y. pseudotuberculosis yopD$_{\Delta150\text{-}170}$ and yopD$_{\Delta207\text{-}227}$ are attenuated during disseminated*

126 *infection.* To address the role of the YopD central region in *Y. pseudotuberculosis* type

127 III secretion and virulence, we constructed in frame deletions of YopD amino acids 150-

128 170 and 207-227 in the IP2666 strain background. Olsson *et al*. previously showed that

129 YopD$_{\Delta150\text{-}170}$ and YopD$_{\Delta207\text{-}227}$ mutant proteins exhibit normal stability (Olsson *et al.*,

130 2004). Indeed, we found that our *yopD$_{\Delta150\text{-}170}$* and *yopD$_{\Delta207\text{-}227}$* mutants secreted Yops,

131 including YopD, *in vitro* to the same extent as wildtype *Y. pseudotuberculosis* (Fig. 1).

132

133 To determine if the YopD central region plays a role in yersiniosis, we infected C57Bl/6

134 mice via the intraperitoneal (I.P.) route with wildtype *Y. pseudotuberculosis* (WT) or the

135 *yopD$_{\Delta150\text{-}170}$* and *yopD$_{\Delta207\text{-}227}$* mutants. Four days post-inoculation, spleens and livers

136 were harvested and bacterial load assessed (Fig. 2). The *yopD$_{\Delta150\text{-}170}$* and *yopD$_{\Delta207\text{-}227}$*

137 mutants had 50 to 250-fold fewer CFUs, respectively, in the spleen and 45 to 65-fold

138 fewer CFUs, respectively, in the liver compared to WT. This suggests that YopD$_{150\text{-}170}$

139 and YopD$_{207\text{-}227}$ carry out one or more functions important for *Y. pseudotuberculosis*

140 disseminated infection.

141

142 *Y. pseudotuberculosis yopD$_{\Delta150\text{-}170}$ and yopD$_{\Delta207\text{-}227}$ exhibit normal pore formation in*

143 *macrophages.* YopD is required to form pores in host cells, facilitating Yop translocation

144   across the host membrane (Neyt C and G Cornelis, 1999). While *yopD*$_{\Delta 150\text{-}170}$ and

145   *yopD*$_{\Delta 207\text{-}227}$ mutants were previously found to disrupt the membrane of red blood cells

146   (RBCs) to a similar extent as *Yersinia* expressing wildtype YopD (Olsson et al. 2004),

147   RBCs are not a physiologically relevant cell type for the *Yersinia* T3SS and differences

148   in pore formation between RBCs and nucleated cells have been described (Kwuan *et*

149   *al.*, 2013). To determine if the *yopD*$_{\Delta 150\text{-}170}$ and *yopD*$_{\Delta 207\text{-}227}$ mutants were capable of

150   disrupting host membranes of physiologically relevant nucleated cells (Durand *et al.*,

151   2010), we measured 2,7-biscarboxyethyl-5(6)-carboxyfluorescein (BCECF) release from

152   macrophages one hour post-inoculation with WT, YopD mutant strains, or a Δ*yscNU*

153   strain unable to form the T3SS apparatus (Fig. 3A). These strains lacked *yopHEMOJN*,

154   as BCECF release is blocked by the presence of effector proteins and the regulatory

155   protein YopN (Marenne, 2003). We observed no difference in BCECF release relative to

156   the parental strain (Fig. 3A and Fig. S1). To further validate this result, we employed an

157   independent pore formation assay that measures the entry of ethidium bromide (EtBr)

158   inside infected macrophages by fluorescence microscopy (Fig. 3B). Once again, we

159   found no difference in the capacity of either the *yopD*$_{\Delta 150\text{-}170}$ or *yopD*$_{\Delta 207\text{-}227}$ mutant to

160   form pores in macrophages relative to the parental strain two hours post-inoculation, the

161   earliest time point EtBr entry can be detected for the positive control (data not shown).

162   Taken together, these findings indicate that the virulence attenuation of the *yopD*$_{\Delta 150\text{-}170}$

163   and *yopD*$_{\Delta 207\text{-}227}$ mutants does not stem from a defect in T3SS-mediated pore formation.

164

165   *Y. pseudotuberculosis yopD*$_{\Delta 150\text{-}170}$ *and yopD*$_{\Delta 207\text{-}227}$ *exhibit impaired translocation into*

166   *host cells.* The virulence defects displayed by the *yopD*$_{\Delta 150\text{-}170}$ and *yopD*$_{\Delta 207\text{-}227}$ mutants

167   suggest that T3SS function may be deficient in these strains. As both YopD mutants

168   displayed normal Yop secretion and macrophage pore formation by two independent

169   assays, we hypothesized that a Yop translocation defect could underlie the *in vivo*

170   phenotype. A previous report described the translocation capacity of *Y.*

171   *pseudotuberculosis* YPIII *yopD$_{\Delta150\text{-}170}$ and yopD$_{\Delta207\text{-}227}$* mutants as being comparable to

172   WT (Olsson *et al.*, 2004). However, these experiments were based on indirect

173   measurement of effector protein translocation, such as cell rounding (Olsson *et al.*,

174   2004). We took a more direct approach by measuring the translocation of plasmid-

175   encoded Yop-β-lactamase (Yop-Bla) reporter proteins into mammalian cells loaded with

176   the fluorescent β-lactamase substrate CCF2-AM (Dewoody *et al.*, 2011). *Y.*

177   *pseudotuberculosis* pYopH-Bla, pYopE-Bla, and pYopM-Bla strains were able to

178   secrete YopH-Bla, YopE-Bla, and YopM-Bla *in vitro* (data not shown) and were used to

179   infect CHO cells. Both the *yopD$_{\Delta150\text{-}170}$* and *yopD$_{\Delta207\text{-}227}$* mutants displayed significant

180   defects in translocating Yops compared to the WT strain (Fig. S2).

181

182   *Yersinia* preferentially target neutrophils, macrophages, and dendritic cells *in vivo*

183   through their T3SS (Marketon *et al.*, 2005; Köberle *et al.*, 2009; Durand *et al.*, 2010). To

184   investigate the translocation capacity of the YopD mutants during infection of

185   physiologically relevant cell types, we performed an *ex vivo* translocation assay using

186   primary murine splenocytes, which include macrophages and neutrophils, among other

187   cells. In order to monitor membrane integrity, single cell suspensions of splenocytes

188   from naïve mice were loaded with CCF2-AM, infected with different *Yersinia* reporter

189   strains for one hour, and analyzed by flow cytometry for green (uncleaved CCF2) and

8

190   blue (cleaved CCF2) fluorescence (Fig. 4A, representative flow cytometry gating). The

191    $yopD_{\Delta150-170}$ mutant translocated YopE-Bla and YopM-Bla into 37% and 24% fewer total

192   splenocytes, respectively, relative to the strains carrying WT YopD (Fig. 4B). Likewise,

193   the $yopD_{\Delta207-227}$ mutant also exhibited a translocation defect as it injected YopE-Bla and

194   YopM-Bla into 30% to 33% fewer total splenocytes, respectively (Fig. 4B). In contrast,

195   we did not detect a defect in YopH-Bla translocation for either of the $yopD$ mutants.

196   However, when we stained these infected splenocytes with antibodies to cell surface

197   markers, we found that both the $yopD_{\Delta150-170}$ and $yopD_{\Delta207-227}$ mutants were impaired at

198   translocating YopH-Bla, YopE-Bla, and YopM-Bla into Gr-1$^+$/CD11b$^+$ cells (referred to

199   here as neutrophils, see Materials and Methods) by approximately 30 to 41% relative to

200   WT (Fig. 5A). Analysis of CD11b$^+$/Gr-1$^-$ cells (referred to here as macrophages, see

201   Materials and Methods) showed that the $yopD_{\Delta150-170}$ and $yopD_{\Delta207-227}$ mutants exhibit a

202   similar translocation defect of 42 to 48% for YopE-Bla cargo (Fig. 5B). Thus, in addition

203   to exhibiting significant translocation deficiencies when a pure culture of CHO cells is

204   the target, the $yopD$ mutants also display substantial defects in Yop translocation when

205   faced with a heterogeneous host cell population, including phagocytic cells. These

206   findings suggest that $YopD_{150-170}$ and $YopD_{207-227}$ are important for efficient delivery of

207   Yops into relevant host cell types such as phagocytes.

208

209   *Y. pseudotuberculosis yopD$_{\Delta150-170}$ and yopD$_{\Delta207-227}$ are defective in inhibiting reactive*

210   *oxygen species production by phagocytes.* The $yopD_{\Delta150-170}$ and $yopD_{\Delta207-227}$ mutants

211   were particularly defective in translocating Yops into neutrophils (Fig. 5A). An important

212   host defense function of neutrophils is the generation of ROS, an activity known to be

9

213   inhibited by YopE and YopH (Bliska and Black, 1995; Ruckdeschel *et al.*, 1996;

214   Songsungthong *et al.*, 2010). We hypothesized that the *yopD*$_{\Delta150\text{-}170}$ and *yopD*$_{\Delta207\text{-}227}$

215   mutants would be defective in inhibiting ROS production in neutrophils as a result of

216   decreased YopH and YopE translocation. We measured the ability of *Y.*

217   *pseudotuberculosis* to inhibit phorbol myristate acetate (PMA)-induced reactive oxygen

218   species (ROS) production by differentiated HL-60 (dHL-60) neutrophil-like cells. As

219   previous studies have either infected phagocytes with bacteria, followed by the addition

220   of PMA, or have added PMA simultaneously with the infection, we carried out both

221   approaches. When PMA was added simultaneously with the *Yersinia* to differentiated

222   dHL-60s, WT *Yersinia* inhibited an average of 50% of ROS production while the

223   *yopD*$_{\Delta150\text{-}170}$ and *yopD*$_{\Delta207\text{-}227}$ strains only inhibited an average of 35% and 15%

224   respectively, although only *yopD*$_{\Delta207\text{-}227}$ was significantly defective relative to WT (Fig.

225   6A-B). When dHL-60 cells were infected with bacteria prior to PMA addition, the

226   *yopD*$_{\Delta150\text{-}170}$ and *yopD*$_{\Delta207\text{-}227}$ strains inhibited ROS an average of 80% and 90%

227   respectively, compared to 98% by WT bacteria, although only *yopD*$_{\Delta150\text{-}207}$ was

228   statistically significant for this assay (Fig. 6C-D). We found that absence of YopE alone

229   completely eliminated the ability of *Y. pseudotuberculosis* to inhibit ROS production in

230   dHL-60 cells under these conditions, as cells infected with a Δ*yopE* mutant produced as

231   much or more ROS than a Δ*yopB* mutant incapable of translocating Yops (Fig. 6E-F).

232   Furthermore, *Y. pseudotuberculosis* Δ*yopE*, Δ*yopE*/*yopD*$_{\Delta150\text{-}170}$, and Δ*yopE*/*yopD*$_{\Delta207\text{-}227}$

233   mutants were all significantly defective in their ability to inhibit ROS production (Fig. 6E-

234   F). Taken together, these data indicate that both the *Y. pseudotuberculosis yopD*$_{\Delta150\text{-}170}$

10

235   and *yopD*$_{\Delta207\text{-}227}$ strains are defective in their ability to inhibit ROS production in

236   phagocytes in a YopE-dependent manner.

237

238   *Y. pseudotuberculosis yopD*$_{\Delta150\text{-}170}$ *and yopD*$_{\Delta207\text{-}227}$ *hyperinduce host cell death.*

239   The *Yersinia* effectors YopJ, YopE, and YopM have been implicated in manipulating

240   host cell death pathways (Monack et al1997, Schotte et al 20004, Bergsbaken and

241   Cookson 2009). As we have observed impaired translocation of multiple *Yersinia*

242   effectors in our YopD central region mutants, we characterized how this defect impacts

243   the ability of *Yersinia* to influence host cell death by measuring LDH release. Both the

244   *yopD*$_{\Delta150\text{-}170}$ and *yopD*$_{\Delta207\text{-}227}$ mutants enhanced LDH release in LPS-primed primary

245   BMDMs two to four hours post-inoculation (Fig. 7A), indicating loss of the ability to

246   inhibit host cell death pathways. *Yersinia* strains individually lacking YopM, YopJ, or

247   YopE did not induce significantly more LDH release than WT bacteria (Fig. 7B),

248   indicating redundancy in preventing host cell death following *Yersinia* infection under

249   these conditions. Indeed, *Y. pseudotuberculosis* lacking all T3SS effector proteins

250   (Δ*yopHEMOJ*) induced more rapid and robust LDH release than wildtype bacteria (Fig.

251   7C). Deletion of the YopHEMOJ effector proteins in the *yopD*$_{\Delta150\text{-}170}$ and *yopD*$_{\Delta207\text{-}227}$

252   genetic backgrounds led to similar LDH release kinetics compared to bacteria

253   expressing wildtype YopD, indicating that the increased LDH release associated with

254   the *yopD*$_{\Delta150\text{-}170}$ and *yopD*$_{\Delta207\text{-}227}$ mutations is dependent on effector Yops. These

255   findings support a model in which decreased Yop translocation by the *yopD*$_{\Delta150\text{-}170}$ and

256   *yopD*$_{\Delta207\text{-}227}$ mutants prevents *Yersinia* from blocking host cell death pathways.

257

258   **Discussion**

11

259   The *Yersinia* translocator protein YopD cooperates with YopB to form the pores on host

260   cell membranes necessary for facilitating delivery of T3SS cargo into host cells. Our

261   study investigated the contribution of the poorly-characterized central region of YopD to

262   T3SS function by analyzing two *Y. pseudotuberculosis* mutants carrying targeted

263   deletions within YopD$_{150-170}$ or YopD$_{207-227}$. We found that *Y. pseudotuberculosis*

264   *yopD*$_{\Delta150-170}$ and *yopD*$_{\Delta207-227}$ mutants exhibited normal host membrane pore formation,

265   confirming a previous report that had suggested these regions of YopD are not required

266   for disrupting the host cell membrane (Olsson *et al.*, 2004). However, the *yopD*$_{\Delta150-170}$

267   and *yopD*$_{\Delta207-227}$ mutants displayed an impaired ability to translocate YopH, YopE, and

268   YopM into mammalian cells, including primary murine neutrophils and macrophages.

269   This compromised entry of effector proteins into host cells corresponded with a

270   diminished capacity to carry out effector protein function, such as inhibition of ROS

271   production in neutrophil-like cells and inhibition of macrophage cell death. Consistent

272   with the known contribution of T3SS effector protein translocation to *Yersinia* virulence,

273   the *yopD*$_{\Delta150-170}$ and *yopD*$_{\Delta207-227}$ mutants were attenuated in a mouse model of

274   disseminated infection. These findings suggest that the central region of YopD plays a

275   specific role in facilitating translocation of Yops inside host cells that is genetically

276   separable from its role in forming pores on host cell membranes, contributing to the

277   ability of *Y. pseudotuberculosis* to cause disseminated infection.

278

279   This study joins a growing body of research suggesting that YopD-mediated host

280   membrane disruption and effector protein translocation are genetically separable

281   activities. For example, YopD F280R and V292D point mutations within a C-terminal

282   amphipathic α-helix lead to three to four-fold less red blood cell lysis yet maintain

283   wildtype levels of effector protein translocation, as measured by ExoS delivery into

284   HeLa cells (Costa *et al.*, 2010). In contrast, a YopD mutant lacking the putative

285   transmembrane domain spanning amino acids 128-149 displays a detectable, albeit two

286   to four-fold diminished, ability to disrupt macrophage membranes but completely fails to

287   translocate a Yop-Bla construct into CHO cells (Olsson *et al.*, 2004; Kwuan *et al.*, 2013).

288   In this report, we show that YopD mutants lacking amino acids 150-170 or 207-227

289   have no discernible defect in disrupting macrophage membranes (Fig. 3), but have

290   diminished capacity to translocate multiple Yop-Bla constructs into a variety of cell

291   types. Thus, YopD-mediated pore formation and effector Yop translocation do not

292   completely correlate, suggesting that YopD may contribute to effector Yop delivery into

293   host cells through a mechanism distinct from interacting with YopB and the host

294   membrane to form a translocation pore. Secondary structure analysis has revealed that

295   a YopD fragment spanning amino acids 150-278 converts between α-helical and

296   random coil states at a neutral pH upon temperature variation, perhaps reflecting a

297   conformational change important for type III secretion of effectors (Raab and Swietnicki,

298   2008; Dohlich *et al.*, 2014). Future advances on the structure of YopD and the LcrV-

299   YopBD translocon will greatly aid in our ability to determine the mechanistic basis for

300   how this region of YopD impacts Yop translocation.

301

302   *Yersinia* preferentially target neutrophils, macrophages, and dendritic cells *in vivo*

303   through their T3SS (Marketon *et al.*, 2005; Köberle *et al.*, 2009; Durand *et al.*, 2010).

304   Both the *yopD*$_{\Delta 150-170}$ and *yopD*$_{\Delta 207-227}$ mutants were impaired for injection of YopH-Bla,

305   YopE-Bla, and YopM-Bla into neutrophils, but only failed to translocate YopE-Bla at WT

306   levels in macrophages. YopE is known to modulate translocation of other Yops and

307   *Yersinia* strains lacking YopE exhibit Yop hyper-translocation (Aili *et al.*, 2008; Mejía *et*

308   *al.*, 2008). Thus, the decrease in YopE translocation by the *yopD* mutants may lead to

309   an increase in delivery of other Yop effectors. It is possible that the effect that

310   decreased YopE translocation may have on YopH-Bla and YopM-Bla injection into

311   macrophages may be greater than the direct contribution of the YopD central region to

312   YopH-Bla and YopM-Bla translocation.

313

314   One established function of YopE is its ability to inhibit ROS production in neutrophils

315   and macrophages (Bliska and Black, 1995; Ruckdeschel *et al.*, 1996; Songsungthong *et*

316   *al.*, 2010). Indeed, both the $yopD_{\Delta150\text{-}170}$ and $yopD_{\Delta207\text{-}227}$ mutants were defective in

317   translocation of YopE-Bla into primary neutrophils and failed to inhibit ROS production

318   to WT levels in dHL-60 neutrophil-like cells. The defect exhibited by the $yopD_{\Delta150\text{-}170}$

319   mutant was most apparent when dHL-60s were infected with *Yersinia* for an hour,

320   followed by PMA addition to induce ROS production (Fig. 6C-D). Conversely, the

321    $yopD_{\Delta207\text{-}227}$ mutant was more impaired at inhibiting ROS production when *Yersinia* and

322   PMA were added to dHL-60s simultaneously (Fig. 6A-B), possibly reflecting subtle

323   differences between the two YopD mutants. One possible explanation for this result is

324   that the $yopD_{\Delta207\text{-}227}$ mutant may be more defective than the $yopD_{\Delta150\text{-}170}$ mutant in

325   YopE translocation and subsequent ROS inhibition within the first 30 minutes of dHL-60

326   cell infection (Fig. 6AB), but is ultimately capable of translocating higher levels of YopE

327   into these target cells by one hour post-inoculation compared to the $yopD_{\Delta150\text{-}170}$ mutant

14

328   (Fig. 6CD). Taken together, however, these findings suggest that the YopD central

329   region is important for robust YopE translocation and effector function in innate immune

330   cells. The ability of *Yersinia* to inhibit ROS production in our experimental setup was

331   completely dependent on YopE (Fig. 6EF). While the effector protein YopH is also

332   known to inhibit ROS production in neutrophils, this has only been shown for the

333   oxidative burst following Fc receptor engagement (Bliska and Black, 1995; Ruckdeschel

334   *et al.*, 1996). Therefore, because the bacteria in our experiment were not opsonized, the

335   ROS production we observed was Fc receptor independent and therefore not affected

336   by YopH activity.

337

338   Several *Yersinia* effector proteins, YopJ, YopE, and YopM, have been shown to

339   modulate host cell death pathways (Monack *et al.*, 1997; Bergsbaken and Cookson,

340   2007; Larock and Cookson, 2012). We found that both the $yopD_{\Delta150-170}$ and $yopD_{\Delta207-227}$

341   mutants hyperinduced macrophage cell death relative to the parental strain, but only in

342   a genetic background encoding the YopHEMOJ effector proteins (Fig. 7AC).

343   Collectively, these data suggest that decreased delivery of YopJ, YopE, and/or YopM

344   prevents full repression of host cell death in the $yopD_{\Delta150-170,}$ and $yopD_{\Delta207-227}$ mutants.

345

346   YopJ is required for induction of apoptosis in naïve macrophages, as *Yersinia* mutants

347   lacking YopJ fail to induce similar levels of apoptosis as WT *Yersinia* (Monack *et al.*,

348   1997). In addition, increased secretion of YopJ results in elevated host cell death

349   (Brodsky and Medzhitov, 2008). Under the assumption that the YopD central region

350   mutants translocate less YopJ as they do other T3SS cargo, these data suggest that

15

351   YopJ-mediated apoptosis is not responsible for driving the increased host cell death

352   triggered by the *yopD* central region mutants. However, Viboud and Bliska showed that

353   a *Y. pseudotuberculosis* YopE mutant exhibited elevated LDH release in HeLa cells

354   (Viboud and Bliska, 2001). This study went on to show that in the absence of YopE,

355   localized actin polymerization is not inhibited, leading to increased pore formation and

356   membrane damage (Viboud and Bliska, 2001). Furthermore, YopE inactivation of Rac1

357   is responsible for the observed LDH release and HeLa cell cytotoxicity (Aili *et al.*, 2006).

358   As both the *yopD*$_{\Delta 150\text{-}170,}$ and *yopD*$_{\Delta 207\text{-}227}$ mutants were defective in translocation of

359   YopE into macrophages, it is possible that this insufficient YopE delivery leads to

360   elevated LDH release (Fig. 7A).

361

362   The *Yersinia* effector protein YopM was recently shown to have a significant impact on

363   host cell death. LaRock and Cookson demonstrated that YopM inhibits caspase-1, a cell

364   death protease important in mediating pyroptosis (Larock and Cookson, 2012). The

365   *yopD*$_{\Delta 150\text{-}170,}$ and *yopD*$_{\Delta 207\text{-}227}$ mutants had a 33% and 49% YopM translocation defect

366   during infection of spleen-derived macrophages, but this was not statistically significant

367   (Fig. 5B). It is possible that decreased YopM translocation inside bone marrow-derived

368   macrophages is significant and contributed to hyperinduction of host cell death in that

369   cell type (Fig. 7A). However, the cell death we observed during infection of activated

370   macrophages with WT *Y. pseudotuberculosis* or the *yopD* mutants was not caspase-1

371   dependent (data not shown). Interestingly, several groups have recently characterized a

372   caspase-1 independent, caspase-11 dependent form of cell death that occurs in

373   response to Gram-negative bacteria (Casson *et al.*, 2013; Case *et al.*, 2013; Aachoui *et*

16

374   *al.*, 2013). Indeed, pyroptosis in response to a *Y. pseudotuberculosis yopM* mutant was

375   recently shown to be partially dependent on capaspe-11 (Chung *et al.*, 2014). Taken

376   together, these results suggest that decreased delivery of YopE and YopM by the

377   *yopD*$_{\Delta150\text{-}170,}$ and *yopD*$_{\Delta207\text{-}227}$ mutants may prevent the bacteria from fully silencing host

378   cell death pathways.

379

380   YopD is known to interact with a range of *Yersinia* proteins, including several that are

381   required for the optimal translocation of effectors. This includes the T3SS substrate

382   YopK, which regulates control and fidelity of translocation (Holmström *et al.*, 1997;

383   Dewoody *et al.*, 2013). For example, a *Yersinia yopK*-deficient strain hypertranslocates

384   T3SS cargo, including YopD (Holmström *et al.*, 1997; Dewoody *et al.*, 2011). YopK is

385   also known to interact with YopD in host cells, suggesting that YopK may mediate its

386   functions directly via the pore formation complex (Dewoody *et al.*, 2011). We

387   investigated the relationship between the YopD central region mutants and YopK by

388   measuring translocation of YopD-Bla into CHO cells. While we confirmed that a Δ*yopK*

389   mutant hypertranslocated YopD-Bla, WT *Y. pseudotuberculosis* and the *yopD*$_{\Delta150\text{-}170,}$

390   and *yopD*$_{\Delta207\text{-}227}$ mutants translocated very little YopD-Bla (data not shown). Thus, while

391   the central region of YopD is required for robust translocation of T3SS cargo, the

392   mechanism underlying this is independent of YopK.

393

394   YopD has been shown to bind directly to YopE *in vitro* and it is thought that the

395   hydrophobic region of YopD encompassing amino acids 122-151 is required for this

396   interaction (Håkansson *et al.*, 1993; Hartland and Robins-Browne, 1998). While there is

397   no evidence to support whether this interaction has a role in virulence, it does establish

398   a unique relationship between a translocator protein and an effector protein. This

399   hydrophobic region is immediately adjacent to the missing amino acid residues in the

400    $yopD_{\Delta150-170}$ *Y. pseudotuberculosis* mutant and slightly upstream of those missing in the

401    $yopD_{\Delta207-227}$ *Y. pseudotuberculosis* mutant. Therefore, one possibility is that $YopD_{150-170}$

402   and $YopD_{207-227}$ contribute to YopE binding during translocation. However, we view this

403   mechanism as unlikely because our data shows that the YopD central region mutants

404   exhibit a broader translocation defect impacting multiple Yop effectors.

405

406   *Y. pseudotuberculosis* mutants lacking *yopH*, *yopE*, or *yopM* display significant

407   virulence defects in the spleen and liver (Logsdon and Mecsas, 2003; Trülzsch *et al.*,

408   2004; Ye *et al.*, 2011; LaRock and Cookson, 2012). The $yopD_{\Delta150-170}$ and $yopD_{\Delta207-227}$

409   mutants exhibited YopH, YopE, and YopM translocation defects into, and decreased

410   Yop activity in, phagocytic cells, paired with a significant virulence defect in both the

411   spleen and liver during mouse infection. Collectively, these data suggest that decreased

412   delivery of YopH, YopE, YopM, and possibly other Yops, inside physiologically relevant

413   host cells prevents *Yersinia* from sufficiently dampening host defenses and efficiently

414   colonizing deep tissue sites. We attempted to test this hypothesis directly by inhibiting

415   ROS production with the NADPH oxidase inhibitor acetovanillone during *Y.*

416   *pseudotuberculosis yopD*$_{\Delta207-227}$ mutant infection. The acetovanillone-treated mice had

417   approximiately ten-fold higher CFU in the spleens of mice compared to control animals,

418   but this difference was not statistically significant (p=0.052, data not shown). This

419   incomplete rescue is not surprising given that we expect the YopD mutant virulence

18

420   defect to result from decreased translocation of multiple effector proteins, and not just

421   YopE/H-mediated inhibition of ROS production *in vivo*. Thus, we would expect that full

422   rescue of the *yopD* central region mutant virulence defect would only be acheived

423   through compensation for the activity of each hypotranslocated Yop.

424

425   In conclusion, we characterized two *Yersinia* mutants, *yopD*$_{\Delta150\text{-}170}$ and *yopD*$_{\Delta207\text{-}227}$, in

426   order to assess the role that the YopD central region plays in *Yersinia* pathogenesis.

427   Despite exhibiting several wildtype *in vitro* phenotypes, both YopD mutants displayed

428   significant translocation defects into host cells, including neutrophils and macrophages.

429   We suggest that these translocation defects prevent effective subversion of host cell

430   defense mechanisms, such as inhibition of ROS production and cell death. Ultimately,

431   the inability of the YopD mutants to effectively manipulate the host immune system

432   manifests in significant virulence attenuation *in vivo*. The complete conservation of

433   YopD$_{150\text{-}170}$ and YopD$_{207\text{-}227}$ in all three pathogenic *Yersinia* species suggests that this

434   central region may ensure optimal translocation of cargo in all three organisms.

435

436

437   **Experimental Procedure**

438

439   *Bacterial growth conditions*

440   *Y. pseudotuberculosis* was grown in 2xYT at 26˚C/shaking overnight. The cultures were

441   back-diluted into low calcium media (2xYT with 20 mM sodium oxalate and 20 mM

442   MgCl$_2$) to an OD$_{600}$ of 0.2 and grown for 1.5 hours at 26°C/shaking followed by 1.5

443   hours at 37°C/shaking to induce Yop synthesis, as previously described (Auerbuch *et*

444   *al.*, 2009). Chloramphenicol was added where necessary to a final concentration of

445   20μg ml^{-1}.

446

447   *Bacterial mutants*

448   The bacterial strains used in this study are listed in Table 1. *Y. pseudotuberculosis*

449   mutants were generated by splicing by overlap extension PCR. The *yopD*$_{\Delta 150\text{-}170}$ and

450   *yopD*$_{\Delta 207\text{-}22}$ mutants were constructed according to the strategy described in Olsson et

451   al (Olsson *et al.*, 2004). Briefly, amplified PCR fragments, encoding ~200-400 bp of

452   homology on either side of the intended mutation, were cloned into pSR47s (Merriam *et*

453   *al.*, 1997; Andrews *et al.*, 1998). Recombinant plasmids were introduced into *E. coli*

454   S17-1λpir and later into *Y. pseudotuberculosis* IP2666. The resulting integrants were

455   plated on sucrose-containing media to identify clones that had lost *sacB*. Kan^{S},

456   sucrose^{R}, congo red-positive colonies were screened by PCR and subsequently

457   sequenced to confirm the presence of the intended mutation.

458

459   The *yopD*$_{\Delta 150\text{-}170}$ and *yopD*$_{\Delta 207\text{-}227}$ mutations was constructed using the internal primers

460   described in (Olsson *et al.*, 2004) along with the external primers 5'-

461   CCAGGGAGGATCCGTTGCATTACTGAG-3' and 5'-

462   CACAACGTCGACTTAACTAATAT-3'. The Δ*yopE* mutation was introduced into *Y.*

463   *pseudotuberculosis* using a suicide plasmid generously provided by Dr. Joan Mecsas

464   (Logsdon and Mecsas, 2003). YopH-Bla, YopE-Bla, and YopM-Bla reporter plasmids, a

465   kind gift from Dr. Melanie Marketon, were electroporated into *Y. pseudotuberculosis*.

466   Single colonies were selected by plating on chloramphenicol and Congo Red plates.

467

468   *Primary cells and cell lines*

469   Primary bone marrow-derived macrophages (BMDM) were prepared as previously

470   described (Auerbuch *et al.*, 2009). Immortalized C57Bl/6 BMDMs were grown in DMEM

471   supplemented with 10% heat-inactivated fetal bovine serum (HyClone) and 2 mM L-

472   glutamine at 37˚C/5% CO_2 (Auerbuch *et al.*, 2009). CHO-K1 (ATCC) cells were

473   maintained in F12K (Cellgro) supplemented with 10% heat-inactivated fetal bovine

474   serum (HyClone) and 2 mM L-glutamine at 37˚C/5% CO_2.

475

476   *In vitro Yop secretion*

477   Visualization of T3SS cargo secreted in broth culture was performed as previously

478   described (Auerbuch *et al.*, 2009). *Y. pseudotuberculosis* low calcium media cultures

479   were grown for 1.5 hrs at 26°C followed by 37°C for 2hrs. Cultures were centrifuged

480   at 16,000 x g for 10 min at room temperature and supernatants transferred to a new

481   eppendorf tube. Trichloroacetic acid was added (10% final) and the mixture vortexed

482   vigorously. Samples were incubated on ice for 20 min and centrifuged at 16,000 x g for

483   15 min at 4°C. The pellet was resuspended in final sample buffer (FSB) plus 20% DTT.

484   Samples were boiled for 5 min prior to running on a 12.5% SDS-PAGE gel. Sample

485   loading was normalized to culture density measured by OD_{600}.

486

487   *BCECF release*

488   BCECF release was performed as previously described (Kwuan *et al.*, 2013). A total of

489    $4x10^5$ immortalized C57Bl/6 BMDMs were plated in each well of a 24 well plate (BD

490   Falcon) in DMEM+10% FBS and incubated overnight. Twenty min prior to infection,

491   BMDMs are washed twice with PBS and incubated with HBSS and 10 µM BCECF-AM

492   (Invitrogen) for 30 min at 37°C/5% CO_2. Cells are washed twice in warmed phenol red-

493   free RPMI. The BCECF-loaded BMDMs were infected at a multiplicity of infection (MOI)

494   of 100 and the infected monolayer was centrifuged at 400xg at 4°C to initiate contact.

495   The cells were then incubated at 37°C/5% CO_2 for 1 hr. Alternatively, 0.09% Triton x-

496   100 was added to the cells 45 min prior to the completion of the experiment to achieve

497   100% BCECF release. The cells were centrifuged for 4 min at 250xg and 140 µL of cell

498   culture supernatant was transferred in triplicate into a 96-well clear-bottom white plate

499   (Corning), and BCECF fluorescence was measured using an excitation wavelength of

500   485 nm and an emission wavelength of 535 nm with a Victor^3 plate reader (Perkin

501   Elmer). The percentage of BCECF release was calculated as [(sample −

502   uninfected)/(Triton X-100 − uninfected)] × 100.

503

504   *Ethidium Bromide Entry*

505   A total of $2×10^4$ immortalized C57BL/6 BMDMs were plated in each well of a 96-well

506   clear-bottom black plate (Corning) in 100 µl DMEM plus 10% FBS and incubated

507   overnight. The cells were infected in triplicate at an MOI of 25 or 100 and centrifuged

508   for 5 min at 750 × *g* at 4°C to initiate contact. The cells were then incubated at 37°C

509   with 5% CO_2 for 2 h. At the end of the incubation period, the medium was aspirated

510   and replaced with 30 µl of PBS containing 25 µg/ml ethidium bromide (EtBr) and

511   12.3 µg/ml Hoechst dye (Fischer). The cell monolayer was visualized using an

512   ImageXpress^{MICRO}automated microscope and MetaXpress analysis software

513   (Molecular Devices). The percentage of EtBr-positive cells was calculated by

514   dividing the number of EtBr-stained cells by the number of Hoechst-stained cells.

515   Data from three separate wells were averaged for each independent experiment.

516

517   *Mouse infections*

518   C57Bl/6 mice were purchased from The Jackson Laboratory. Six to eight week old

519   C57/B6J mice were infected with ~$1x10^3$ *Y. pseudotuberculosis* via intraperitoneal (I.P.),

520   injection as previously described (Auerbuch *et al.*, 2009). Four days post inoculation

521   spleens and livers were harvested, homogenized, and serial dilutions of the

522   homogenate were plated to determine CFU per gram (CFU/g) tissue.

523

524   *Yop-Bla translocation inside CHO-K1 cells with microscopy*

525   A total of $2x10^4$ CHO-K1 cells were plated in each well of a 96-well plate in 100 µL of

526   F12K + 10% FBS and incubated overnight. CHO-K1 cells were infected with the

527   indicated *Y. pseudotuberculosis* β-lactamase reporter strain at an MOI of 10. As an

528   additional negative control, CHO cells were infected with a *Y. pseudotuberculosis* strain

529   expressing a GST-Bla fusion protein (data not shown). Immediately following *Y.*

530   *pseudotuberculosis* addition, the plate was spun at 110 x g for 5 min and incubated at

531   37˚C/5% CO_2 for 2 hours. At 30 min post-inoculation, the supernatant was gently

532   aspirated and replaced with fresh media. Between 30-45 min prior to the end of the

533   infection, CCF2-AM (Invitrogen) was added to each well and the plate incubated at

534 30°C/5% CO_2. At 110 min post infection the media was aspirated and DRAQ5 added to

535 each well. Monolayers were incubated at room temperature for 5 min, washed once with

536 PBS, and visualized using an ImageXpress^{MICRO} automated microscope and

537 MetaXpress analysis software (Molecular Devices).

538

539 *Yop-Bla translocation inside CHO-K1 cells*

540 A total of 1x10^5 CHO-K1 cells were plated in each well of a 24-well plate in 500 µL of

541 F12K + 10% FBS and incubated overnight. CHO-K1 cells were loaded with CCF2-AM

542 (Invitrogen) and the plate incubated at 30°C/5% CO_2 for 30 min prior to infection. CHO-

543 K1 cells were infected with the indicated *Y. pseudotuberculosis* β-lactamase reporter

544 strain at an MOI of 10 or 50. Immediately following *Y. pseudotuberculosis* addition, the

545 plate was spun at 110 x g for 5 min and incubated at 37°C/5% CO_2 for 1 hour.

546 Monolayers were trypsinized and incubated for 5 min at 37°C/5% CO_2. A total of 2x10^6

547 cells were resuspended in 100 µL of FACS Buffer (PBS + 5% FBS). At least 2x10^5 cells

548 were acquired per sample and data was analyzed using FlowJo v8.8.7 software.

549

550 *Yop-Bla translocation inside splenocytes*

551 Spleens were harvested from uninfected 6-8 week old C57Bl/6J mice. To generate

552 single cell suspensions, spleens were placed in a six-well plate containing HBSS with

553 Ca^{2+} and Mg^{2+} and perfused with 400 Mandl units ml^{-1} collagenase D (Roche) followed

554 by a 30 min incubation at 37°C. Cells were passed through a 70 µm strainer and

555 pelleted at 15,800 x g for 5 min. The pellet was resuspended in HBSS with 1mM EDTA

24

556   to halt collagenase activity. Cells were treated with Red Blood Cell Lysis Buffer (Sigma)

557   for 7 min and resuspended in $1x10^7$ cells ml^{-1} of RPMI + 5% FBS.

558

559   Single cell suspensions were loaded with 0.18µg ml^{-1} CCF2-AM for 2 h at 30°C,

560   according to the manufacturer's recommendations (Invitrogen). RPMI without phenol

561   red was substituted for Solution C to prevent autofluorescence interference during flow

562   cytometry. Cells were then infected with the indicated *Y. pseudotuberculosis* β-

563   lactamase reporter strains for 1 hr at an MOI of 1 and incubated at 37°C/5% CO_2. A

564   total of $2x10^6$ cells were resuspended in 100 µL of FACS Buffer (PBS + 5% FBS) and

565   blocked with Mouse BD Fc Block^{TM} (BD) for 10 min at 4°C. Cells were incubated in 100

566   µL of FACS buffer containing Gr-1-APC-Cy7 and CD11b-PE-Cy5 (eBioscience) for 30

567   min at 4°C. Samples were washed once with FACS Buffer, centrifuged at 15,800 x g,

568   resuspended in FACS buffer and analyzed on an LSRII flow cytometer (Becton

569   Dickson). At least $2x10^5$ cells were acquired per sample and data was analyzed using

570   FlowJo v8.8.7 software. Cells that were not infected or labeled were used as negative

571   controls. Fluoresence Minus One (FMO) controls were used to establish gating

572   strategies.

573

574   CD11b is expressed on murine monocytes, granulocytes (including neutrophils), and

575   NK cells (Ault and Springer, 1981; Chiossone *et al.*, 2009), while Gr-1 is found on

576   granulocytes as well as subpopulations of monocyte-type ring cells (Lagasse and

577   Weissman, 1996; Biermann *et al.*, 1999). We refer to Gr-1$^+$/CD11b$^+$ cells as neutrophils

578   and Gr-1$^-$/CD11b$^+$ cells as macrophages, consistent with previous reports (Durand *et*

579   *al.*, 2010).

580

581   *Reactive oxygen species detection*

582   HL-60 cells were cultured in IMDM with 20% FBS. HL-60 cells were differentiated into

583   neutrophil-like HL-60 cells (dHL-60s) by culturing them in RPMI 1640 with 15% FBS and

584   1.3% DMSO for 5-6 days (Millius and Weiner, 2010). Cells were plated at 1x10^5

585   cells/well in HBSS in a 96-well white clear bottom tissue culture plates (Corning) and

586   incubated overnight at 37˚C/5% CO_2. Prewarmed HBSS without phenol red containing

587   100 µM luminol and 1 µg µl^{-1} horseradish peroxidase was added to the dHL-60s for 30-

588   60 min at 37˚C/5% CO_2. dHL-60s were infected at MOI 15 with the indicated strain for 1

589   hr in HBSS without phenol red. 1µg ml^{-1} PMA in HBSS without phenol red was added to

590   induce ROS production. Alternatively, dHL-60s were infected at MOI 15 with the

591   indicated strain with 1µg ml^{-1} PMA in HBSS without phenol red simultaneously.

592   Luminescence readings were taken immediately after infection for 30 min using a plate

593   reader (Perkin-Elmer).

594

595   *LDH Release*

596   LDH experiments were performed as previously described with the following

597   modifications (Kwuan et al. 2012). A total of 2.5 × 10^6 primary C57BL/6 BMDMs were

598   plated in each well of a 6-well plate (BD Falcon) in 2 ml DMEM plus 10% FBS and

599   incubated overnight. The cells were primed for with LPS from *Salmonella typhimurium*

600   at a final concentration of 100 ng/ml for approximately 18 hours. 200 microliters of

26

601 supernatant was transferred to an Eppendorf tube every hour for 4 h. After the last time

602 point, the cells were freeze-thawed to achieve full lactate dehydrogenase (LDH)

603 release. Supernatants were centrifuged for 1 min at 13,000 rpm, and 50 µl was

604 transferred to a 96-well clear-bottom white plate (Corning). LDH release into the

605 supernatant was measured using the CytoTox 96 nonradioactive cytotoxicity assay

606 according to the manufacturer's instructions (Promega). LDH release as a result of

607 freeze-thaw was set at 100% for each sample.

608

609 *Statistical analysis*

610 Plotting of data and statistical analysis were performed using KaleidaGraph software.

611 Statistical significance was determined by the unpaired Wilcoxon test for animal

612 experiments, one-way ANOVA with Bonferonni's post-hoc test for ethidium bromide

613 entry, and one-way ANOVA with Tukey post-hoc test for all other experiments.

614

615 **Acknowledgements**

625

28

626   References

627   Aachoui, Y., Leaf, I.A., Hagar, J.A., Fontana, M.F., Campos, C.G., Zak, D.E., *et al.*
628   (2013) Caspase-11 protects against bacteria that escape the vacuole. *Science* **339**:
629   975–8.

630   Aili, M., Isaksson, E.L., Carlsson, S.E., Wolf-Watz, H., Rosqvist, R., and Francis, M.S.
631   (2008) Regulation of *Yersinia* Yop-effector delivery by translocated YopE. *Int J Med*
632   *Microbiol* **298**: 183–192.

633   Aili, M., Isaksson, E.L., Hallberg, B., Wolf-Watz, H., and Rosqvist, R. (2006) Functional
634   analysis of the YopE GTPase-activating protein (GAP) activity of *Yersinia*
635   *pseudotuberculosis*. *Cell Microbiol* **8**: 1020–1033.

636   Andrews, H.L., Vogel, J.P., and Isberg, R.R. (1998) Identification of linked *Legionella*
637   *pneumophila* genes essential for intracellular growth and evasion of the endocytic
638   pathway. *Infect Immun* **66**: 950–958.

639   Auerbuch, V., Golenbock, D.T., and Isberg, R.R. (2009) Innate immune recognition of
640   *Yersinia pseudotuberculosis* type III secretion. *PLoS Pathog* **5**: e1000686.

641   Ault, K.A., and Springer, T.A. (1981) Cross-reaction of a rat-anti-mouse phagocyte-
642   specific monoclonal antibody (anti-Mac-1) with human monocytes and natural killer
643   cells. *J Immunol* **126**: 359–64.

644   Balada-Llasat, J.-M., and Mecsas, J. (2006) *Yersinia* has a tropism for B and T cell
645   zones of lymph nodes that is independent of the type III secretion system. *PLoS Pathog*
646   **2**: e86.

647   Bergsbaken, T., and Cookson, B.T. (2007) Macrophage activation redirects *Yersinia*-
648   infected host cell death from apoptosis to caspase-1-dependent pyroptosis. *PLoS*
649   *Pathog* **3**: e161.

650   Bergsbaken, T., Fink, S.L., and Cookson, B.T. (2009) Pyroptosis: host cell death and
651   inflammation. *Nat Rev Microbiol* **7**: 99–109.

652   Biermann, H., Pietz, B., Dreier, R., Schmid, K.W., Sorg, C., and Sunderkötter, C. (1999)
653   Murine leukocytes with ring-shaped nuclei include granulocytes, monocytes, and their
654   precursors. *J Leukoc Biol* **65**: 217–31.

655   Bliska, J.B., and Black, D.S. (1995) Inhibition of the Fc receptor-mediated oxidative
656   burst in macrophages by the *Yersinia pseudotuberculosis* tyrosine phosphatase. *Infect*
657   *Immun* **63**: 681–5.

658 Bliska, J.B., Guan, K.L., Dixon, J.E., and Falkow, S. (1991) Tyrosine phosphate
659 hydrolysis of host proteins by an essential *Yersinia* virulence determinant. *Proc Natl*
660 *Acad Sci U S A* **88**: 1187–1191.

661 Brodsky, I.E., and Medzhitov, R. (2008) Reduced secretion of YopJ by *Yersinia* limits in
662 vivo cell death but enhances bacterial virulence. *PLoS Pathog* **4**: e1000067.

663 Case, C.L., Kohler, L.J., Lima, J.B., Strowig, T., Zoete, M.R. de, Flavell, R.A., *et al.*
664 (2013) Caspase-11 stimulates rapid flagellin-independent pyroptosis in response to
665 *Legionella pneumophila*. *Proc Natl Acad Sci U S A* **110**: 1851–6.

666 Casson, C.N., Copenhaver, A.M., Zwack, E.E., Nguyen, H.T., Strowig, T., Javdan, B., *et*
667 *al.* (2013) Caspase-11 activation in response to bacterial secretion systems that access
668 the host cytosol. *PLoS Pathog* **9**: e1003400.

669 Chiossone, L., Chaix, J., Fuseri, N., Roth, C., Vivier, E., and Walzer, T. (2009)
670 Maturation of mouse NK cells is a 4-stage developmental program. *Blood* **113**: 5488–
671 96.

672 Chung, L.K., Philip, N.H., Schmidt, V.A., Koller, A., Strowig, T., Flavell, R.A., *et al.*
673 (2014) IQGAP1 is important for activation of caspase-1 in macrophages and is targeted
674 by *Yersinia pestis* type III effector YopM. *MBio* **5**: e01402–14.

675 Cornelis, G.R. (2006) The type III secretion injectisome. *Nat Rev Microbiol* **4**: 811–25.

676 Costa, T.R.D., Edqvist, P.J., Bröms, J.E., Ahlund, M.K., Forsberg, A., and Francis, M.S.
677 (2010) YopD self-assembly and binding to LcrV facilitate type III secretion activity by
678 *Yersinia pseudotuberculosis*. *J Biol Chem* **285**: 25269–84.

679 Cover, T., and Aber, R. (1989) *Yersinia enterocolitica* — NEJM. *New Engl J Medicicne*
680 321: 16–24.

681 Dewoody, R., Merritt, P.M., Houppert, A.S., and Marketon, M.M. (2011) YopK regulates
682 the *Yersinia pestis* type III secretion system from within host cells. *Mol Microbiol* **79**:
683 1445–61.

684 Dewoody, R., Merritt, P.M., and Marketon, M.M. (2013) YopK controls both rate and
685 fidelity of Yop translocation. *Mol Microbiol* **87**: 301–17.

686 Diepold, A., Amstutz, M., Abel, S., Sorg, I., Jenal, U., and Cornelis, G.R. (2010)
687 Deciphering the assembly of the *Yersinia* type III secretion injectisome. *EMBO J* **29**:
688 1928–1940.

689 Durand, E.A., Maldonado-Arocho, F.J., Castillo, C., Walsh, R.L., and Mecsas, J. (2010)
690 The presence of professional phagocytes dictates the number of host cells targeted for
691 Yop translocation during infection. *Cell Microbiol* **12**: 1064–82.

692   Håkansson, S., Bergman, T., Vanooteghem, J.C., Cornelis, G., and Wolf-Watz, H.
693   (1993) YopB and YopD constitute a novel class of *Yersinia* Yop proteins. *Infect Immun*
694   **61**: 71–80.

695   Hartland, E.L., and Robins-Browne, R.M. (1998) In vitro association between the
696   virulence proteins, YopD and YopE, of *Yersinia enterocolitica*. *FEMS Microbiol Lett* **162**:
697   207–213.

698   Holmström, A., Petterson, J., Rosqvist, R., Håkansson, S., Tafazoli, F., Fällman, M., *et*
699   *al.* (1997) YopK of *Yersinia pseudotuberculosis* controls translocation of Yop effectors
700   across the eukaryotic cell membrane. *Mol Microbiol* **24**: 73–91.

701   Keith, K.E., Hynes, D.W., Sholdice, J.E., and Valvano, M.A. (2009) Delayed association
702   of the NADPH oxidase complex with macrophage vacuoles containing the opportunistic
703   pathogen *Burkholderia cenocepacia*. *Microbiology* **155**: 1004–1015.

704   Köberle, M., Klein-Günther, A., Schütz, M., Fritz, M., Berchtold, S., Tolosa, E., *et al.*
705   (2009) *Yersinia enterocolitica* targets cells of the innate and adaptive immune system by
706   injection of Yops in a mouse infection model. *PLoS Pathog* **5**: e1000551.

707   Kwuan, L., Adams, W., and Auerbuch, V. (2013) Impact of Host Membrane Pore
708   Formation by the *Yersinia pseudotuberculosis* Type III Secretion System on the
709   Macrophage Innate Immune Response. *Infect Immun* **81**: 905–14.

710   Lagasse, E., and Weissman, I.L. (1996) Flow cytometric identification of murine
711   neutrophils and monocytes. *J Immunol Methods* **197**: 139–150.

712   Larock, C.N., and Cookson, B.T. (2012) The *Yersinia* virulence effector YopM binds
713   caspase-1 to arrest inflammasome assembly and processing. *Cell Host Microbe* **12**:
714   799–805.

715   Logsdon, L.K., and Mecsas, J. (2003) Requirement of the *Yersinia pseudotuberculosis*
716   Effectors YopH and YopE in Colonization and Persistence in Intestinal and Lymph
717   Tissues. *Infect Immun* **71**: 4595–4607.

718   Marenne, M. (2003) Genetic analysis of the formation of the Ysc–Yop translocation pore
719   in macrophages by *Yersinia enterocolitica*: role of LcrV, YscF and YopN. *Microb Pathog*
720   **35**: 243–258.

721   Marketon, M.M., DePaolo, R.W., DeBord, K.L., Jabri, B., and Schneewind, O. (2005)
722   Plague bacteria target immune cells during infection. *Science* **309**: 1739–41.

723   Mejía, E., Bliska, J.B., and Viboud, G.I. (2008) *Yersinia* controls type III effector delivery
724   into host cells by modulating Rho activity. *PLoS Pathog* **4**: e3.

725 Merriam, J.J., Mathur, R., Maxfield-Boumil, R., and Isberg, R.R. (1997) Analysis of the
726 *Legionella pneumophila fliI* gene: intracellular growth of a defined mutant defective for
727 flagellum biosynthesis. *Infect Immun* **65**: 2497–2501.

728 Millius, A., and Weiner, O.D. (2010) Manipulation of neutrophil-like HL-60 cells for the
729 study of directed cell migration. *Methods Mol Biol* **591**: 147–158.

730 Monack, D.M., Mecsas, J., Ghori, N., and Falkow, S. (1997) *Yersinia* signals
731 macrophages to undergo apoptosis and YopJ is necessary for this cell death. *Proc Natl*
732 *Acad Sci U S A* **94**: 10385–10390.

733 Montagner, C., Arquint, C., and Cornelis, G.R. (2011) Translocators YopB and YopD
734 from *Yersinia enterocolitica* Form a Multimeric Integral Membrane Complex in
735 Eukaryotic Cell Membranes. *J Bacteriol* **193**: 6923–6928.

736 Neyt, C., and Cornelis, G.R. (1999) Insertion of a Yop translocation pore into the
737 macrophage plasma membrane by *Yersinia enterocolitica*: requirement for translocators
738 YopB and YopD, but not LcrG. *Mol Microbiol* **33**: 971–981.

739 Olsson, J., Edqvist, P.J., Bröms, J.E., Forsberg, A., Wolf-Watz, H., and Francis, M.S.
740 (2004) The YopD translocator of *Yersinia pseudotuberculosis* is a multifunctional protein
741 comprised of discrete domains. *J Bacteriol* **186**: 4110–23.

742 Pettersson, J., Nordfelth, R., Dubinina, E., Bergman, T., Gustafsson, M., Magnusson,
743 K.E., and Wolf-Watz, H. (1996) Modulation of Virulence Factor Expression by Pathogen
744 Target Cell Contact. *Science (80-)* **273**: 1231–1233.

745 Philip, N.H., and Brodsky, I.E. (2012) Cell death programs in *Yersinia* immunity and
746 pathogenesis. *Front Cell Infect Microbiol* **2**: 149.

747 Raab, R., and Swietnicki, W. (2008) *Yersinia pestis* YopD 150-287 fragment is partially
748 unfolded in the native state. *Protein Expr Purif* **58**: 53–60.

749 Rosqvist, R., Magnusson, K.E., and Wolf-Watz, H. (1994) Target cell contact triggers
750 expression and polarized transfer of *Yersinia* YopE cytotoxin into mammalian cells.
751 *EMBO J* **13**: 964–72.

752 Ruckdeschel, K., Roggenkamp, A., Schubert, S., and Heesemann, J. (1996) Differential
753 contribution of *Yersinia enterocolitica* virulence factors to evasion of microbicidal action
754 of neutrophils. *Infect Immun* **64**: 724–33.

755 Ryndak, M.B., Chung, H., London, E., and Bliska, J.B. (2005) Role of predicted
756 transmembrane domains for type III translocation, pore formation, and signaling by the
757 *Yersinia pseudotuberculosis* YopB protein. *Infect Immun* **73**: 2433–43.

758   Schotte, P., Denecker, G., Broeke, A. Van Den, Vandenabeele, P., Cornelis, G.R., and
759   Beyaert, R. (2004) Targeting Rac1 by the *Yersinia* effector protein YopE inhibits
760   caspase-1-mediated maturation and release of interleukin-1beta. *J Biol Chem* **279**:
761   25134–42.

762   Segal, A.W. (2005) How neutrophils kill microbes. *Annu Rev Immunol* **23**: 197–223.

763   Songsungthong, W., Higgins, M.C., Rolán, H.G., Murphy, J.L., and Mecsas, J. (2010)
764   ROS-inhibitory activity of YopE is required for full virulence of *Yersinia* in mice. *Cell*
765   *Microbiol* **12**: 988–1001.

766   Takeya, R., and Sumimoto, H. (2003) Molecular mechanism for activation of
767   superoxide-producing NADPH oxidases. *Mol Cells* **16**: 271–277.

768   Trülzsch, K., Sporleder, T., Igwe, E.I., Rüssmann, H., and Heesemann, J. (2004)
769   Contribution of the major secreted yops of *Yersinia enterocolitica* O:8 to pathogenicity in
770   the mouse infection model. *Infect Immun* **72**: 5227–34.

771   Viboud, G.I., and Bliska, J.B. (2001) A bacterial type III secretion system inhibits actin
772   polymerization to prevent pore formation in host cell membranes. *EMBO J* **20**: 5373–
773   5382.

774   Viboud, G.I., and Bliska, J.B. (2005) *Yersinia* outer proteins: role in modulation of host
775   cell signaling responses and pathogenesis. *Annu Rev Microbiol* **59**: 69–89.

776   Ye, Z., Uittenbogaard, A.M., Cohen, D.A., Kaplan, A.M., Ambati, J., and Straley, S.C.
777   (2011) Distinct CCR2(+) Gr1(+) cells control growth of the *Yersinia pestis* ΔyopM
778   mutant in liver and spleen during systemic plague. *Infect Immun* **79**: 674–87.

779

780

781

Strain	Background	Mutation	Reference
Y. pseudotuberculosis			
Wildtype	IP2666	Naturally lacks full length YopT	(Bliska *et al.*, 1991)
Δ*yscNU*	IP2666	Δ*yscNU*	(Balada-Llasat and Mecsas, 2006)
yopD$_{\Delta150-170}$	IP2666	*yopD*$_{\Delta150-170}$	This work
yopD$_{\Delta207-227}$	IP2666	*yopD*$_{\Delta207-227}$	This work
Δ*yopB*	IP2666	*yopB*	This work
WT+YopH-Bla	IP2666	pMM83::*yopH-bla* fusion	This work
yopD$_{\Delta150-170}$+YopH-Bla	IP2666	*yopD*$_{\Delta150-170,}$ pMM83::*yopH-bla* fusion	This work
yopD$_{\Delta207-227}$+YopH-Bla	IP2666	*yopD*$_{\Delta207-227,}$ pMM83::*yopH-bla* fusion	This work
Δ*yopB*+YopH-Bla	IP2666	*yopB::yopH-bla fusion*	This work
WT+YopE-Bla	IP2666	pMM83::*yopE-bla* fusion	This work
yopD$_{\Delta150-170}$+YopE-Bla	IP2666	*yopD*$_{\Delta150-170,}$ pMM83::*yopE-bla* fusion	This work
yopD$_{\Delta207-227}$+YopE-Bla	IP2666	*yopD*$_{\Delta207-227,}$ pMM83::*yopE-bla* fusion	This work
WT+YopM-Bla	IP2666	pMM83::*yopM-bla* fusion	This work
yopD$_{\Delta150-170}$+YopM-Bla	IP2666	*yopD*$_{\Delta150-170,}$ pMM83::*yopM-bla* fusion	This work
yopD$_{\Delta207-227}$+YopM-Bla	IP2666	*yopD*$_{\Delta207-227,}$ pMM83::*yopM-bla* fusion	This work
Δ*yopM*	IP2666	*yopM*	This work
Δ*yopJ*	IP2666	*yopJ*	This work
Δ*yopE*	IP2666	*yopE*	This work
Δ*yopE/ yopD*$_{\Delta150-170}$	IP2666	*yopE/yopD*$_{\Delta150-170}$	This work
Δyop*E/yopD*$_{\Delta207-227}$	IP2666	*yopE/yopD*$_{\Delta207-227}$	This work
Δyop6/Δ*yopN/yopD*$_{\Delta150-170}$	IP2666	*yopHEMOJN/yopD*$_{\Delta150-170}$	This work
Δyop6/Δ*yopN/ yopD*$_{\Delta207-227}$	IP2666	*yopHEMOJN/yopD*$_{\Delta207-227}$	This work

782

783

Figure Legends

Figure 1. Analysis of supernatants containing T3SS cargo secreted by *Y. pseudotuberculosis in vitro*. *Y. pseudotuberculosis* strains were grown under T3SS-inducing conditions and secreted proteins visualized by SDS-PAGE analysis and coomassie blue staining. Wildtype YopD is 33kD, while $YopD_{\Delta150-170}$ and $YopD_{\Delta207-227}$ are ~31 kD. Shown is a representative gel out of three total.

Figure 2. Colonization of the spleen and liver by *Y. pseudotuberculosis* expressing wildtype or mutant YopD. C57Bl/6J mice were infected with $1x10^3$ WT, $yopD_{\Delta150-170}$, or $yopD_{\Delta207-227}$ *Y. pseudotuberculosis* via intraperitoneal injection. Organs were harvested four days post-inoculation and CFU per gram tissue determined. Data from two (*yopD* mutants) to three (WT) independent experiments are shown. Bars indicate the geometric mean; open diamonds indicate that CFU were below the limit of detection. ** $p < 0.005$, *** $p < 0.0001$ using the Wilcoxon-Mann-Whitney non-parametric test.

Figure 3. Analysis of T3SS-mediated pore formation in macrophages. (A) Immortalized bone marrow derived macrophages were loaded with BCECF, infected with *Y. pseudotuberculosis* using centrifugation at an MOI of 100, and BCECF release measured one hour post-inoculation. Shown is the average of five independent experiments ± standard error of the mean (SEM). **(B)** Entry of ethidium bromide (EtBr) inside *Yersinia*-infected immortalized C57BL/6 BMDMs was monitored 2 h

35

807   postinoculation using fluorescence microscopy. The number of EtBr-positive cells

808   out of the total Hoechst-positive cells was quantified 2 h postinoculation. The

809   averages ± SEM from three independent experiments are shown. *, $P \leq 0.05$, and

810   ***, $P \leq 0.0005$, as determined by one-way ANOVA followed by Bonferroni's *post*

811   *hoc* test, where each indicated group was compared to the appropriate negative and

812   positive controls

813

814   **Figure 4. Translocation of YopH-Bla, YopE-Bla, and YopM-Bla reporter proteins**

815   **into splenocytes. (A)** Single cell suspensions of splenocytes were loaded with CCF2

816   and infected with *Y. pseudotuberculosis* carrying YopH-Bla, YopE-Bla, or YopM-Bla at

817   an MOI of one for one hour. Flow cytometry was used to determine the percentage of

818   blue cells. The gating for one representative experiment is shown. **(B)** Translocation of

819   YopH-Bla, YopE-Bla, or YopM-Bla into splenocytes was quantified by flow cytometry.

820   Graphs show the relative % of blue$^+$ splenocytes normalizing to WT+Yop-Bla. The

821   average of two to five independent experiments $\pm$ SEM is shown. * p<0.05, ** p<0.01,

822   *** p<0.005, and **** p<0.0001 using a one-way ANOVA, Post-hoc: Tukey HSD.

823

824   **Figure 5. Translocation of YopH-Bla, YopE-Bla, and YopM-Bla reporter proteins**

825   **into spleen-derived macrophages and neutrophils.** Splenocytes were labeled with

826   cell surface markers to identify macrophages and neutrophils. Neutrophils (Gr-

827   1$^+$CD11b$^+$) and macrophages (CD11b$^+$Gr-1$^-$) were initially gated on CD11b and Gr-1

828   and sub-gated on cleaved CCF2 (blue) and uncleaved CCF2 (green) to identify the % of

829   blue cells within each cell type. Graphs show the relative % of blue$^+$ **(A)** neutrophils and

830   **(B)** macrophages, normalized to WT+Yop-Bla. Shown are the averages from two to four

831   independent experiments ± SEM. * p<0.05, ** p<0.01, *** p<0.005, and **** p<0.0001

832   using a one-way ANOVA, Post-hoc: Tukey HSD.

833

834   **Figure 6. Inhibition of reactive oxygen species production in dHL-60 neutrophil-**

835   **like cells by *Y. pseudotuberculosis*.** Differentiated HL-60 cells (dHL-60) were

836   incubated with luminol and horseradish peroxidase 0.5-1hr prior to infection. PMA plus

837   WT *Y. pseudotuberculosis* (▼), *yopD*$_{\Delta150\text{-}170}$ (●), *yopD*$_{\Delta207\text{-}227}$ (□), Δ*yopB* (○), or PMA

838   alone (▲), or uninfected and untreated (■). **(A-B)** dHL-60s were treated with PMA to

839   induce ROS production and simultaneously infected with the indicated *Y.*

840   *pseudotuberculosis* strain at MOI 15. ROS production was measured in relative light

841   units (RLU) using a plate reader. **(C-D)** dHL-60s were infected with the indicated *Y.*

842   *pseudotuberculosis* strain at MOI 15 for 1 h. PMA was then added to induce ROS

843   production and ROS production monitored using a plate reader. **(E-F)** PMA plus WT *Y.*

844   *pseudotuberculosis* (▼), Δ*yopB* (○), Δ*yopE* (●), Δ*yopE/yopD*$_{\Delta150\text{-}170}$ (□), Δ*yopE/yopD*$_{\Delta207\text{-}}$

845   $_{227}$ (♦), or PMA alone (▲), or uninfected and untreated (■). dHL-60s were infected with

846   the indicated *Y. pseudotuberculosis* strain at MOI 15 for 1 h. PMA was then added to

847   induce ROS production and ROS production monitored using a plate reader. A, C, and

848   E shows the raw data from one biological replicate, while B, D, and F show the

849   normalized average of three independent experiments ± SEM. *=p<0.05, **=p<0.005,

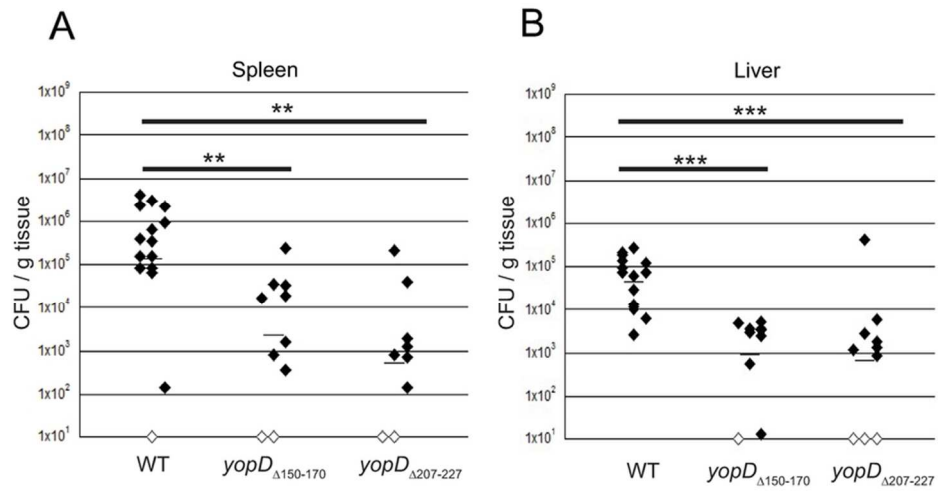850   ***=p<0.0005 using a one-way ANOVA, Post-hoc: Tukey HSD.

851

852   **Figure 7. Inhibition of host cell death in macrophages by *Y. pseudotuberculosis*.**

853   Primary (bone marrow derived macrophages) BMDMs were incubated with LPS for

854   approximately 18 hours and infected with the indicated *Y. pseudotuberculosis* strains.

855   Supernatants were analyzed for (lactate dehydrogenase) LDH release over four hours

856   post-inoculation at one hour intervals. The amount of LDH released from freeze-thaw

857   lysis of the cell monolayer was set at 100%. **(A)** WT *Y. pseudotuberculosis* (▼), *yopD*⁻

858   $_{\Delta150\text{-}170}$ (●), *yopD*$_{\Delta207\text{-}227}$ (□), Δ*yopB* (○), or uninfected and untreated (■). **(B)** WT *Y.*

859   *pseudotuberculosis* (▼), Δ*yopJ* (●), Δ*yopE* (□), Δ*yopM* (▲), or uninfected and untreated

860   (■). (**C**) Δ6 (▼), Δ6/*yopD*$_{\Delta150\text{-}170}$ (●), Δ6/*yopD*$_{\Delta207\text{-}227}$ (□), Δ6/Δ*yopB* (○), or uninfected and

861   untreated (■). The average of three to six independent experiments ± SEM is shown.

862   *=p<0.01, **=p<0.0005, ***=p<0.0001 using a one-way ANOVA, Post-hoc: Tukey HSD.

863

864

38
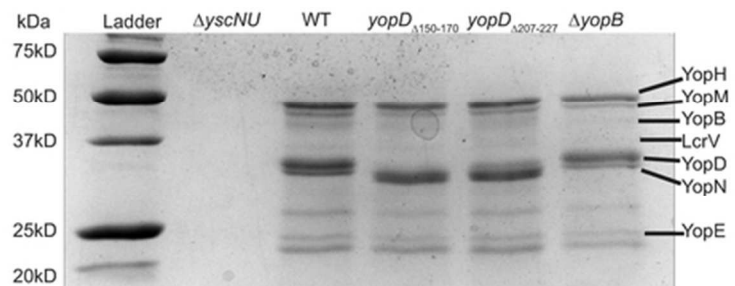
53x15mm (300 x 300 DPI)

82x41mm (300 x 300 DPI)

A

B
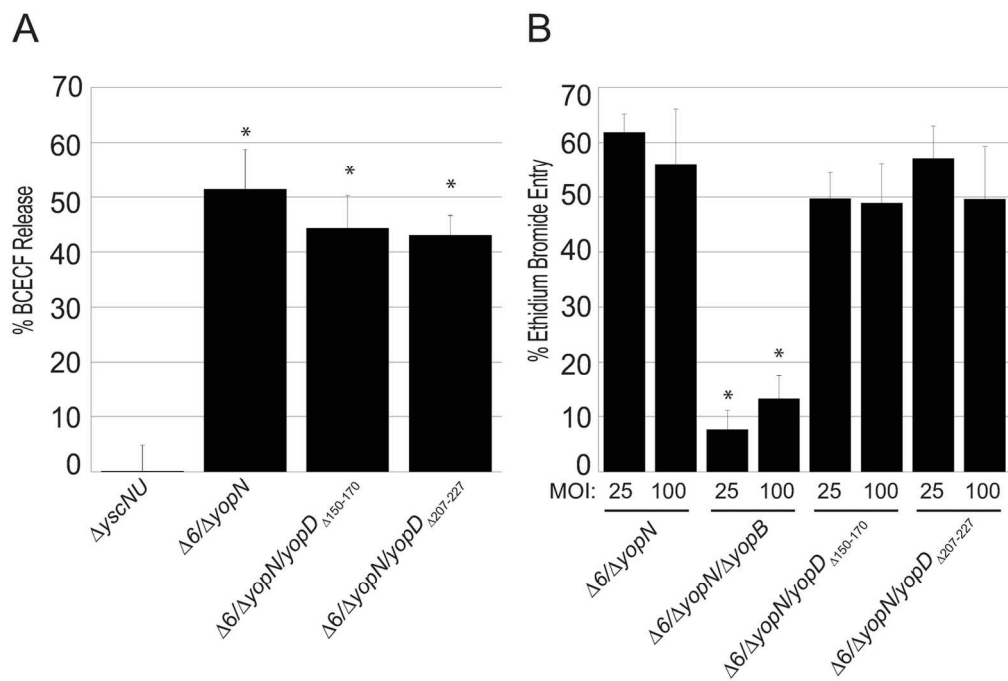
135x113mm (300 x 300 DPI)

view

A

uninfected	ΔyopB	WT	yopD$_{\Delta150-170}$	yopD$_{\Delta207-227}$
0.032%	1.73%	14.5%	10.2%	11.1%

B
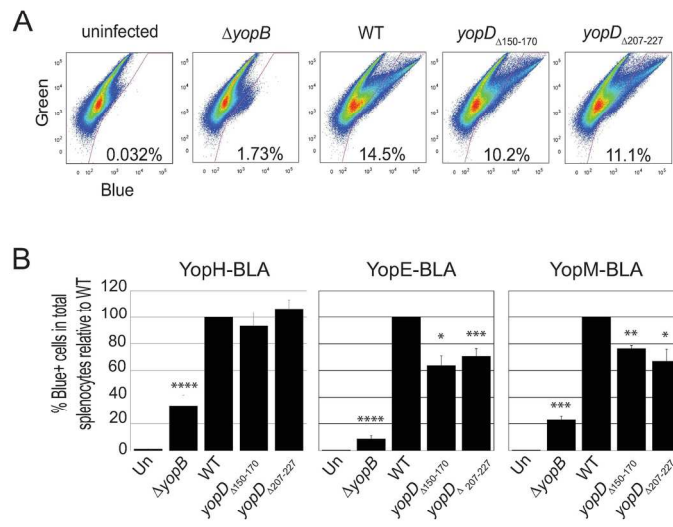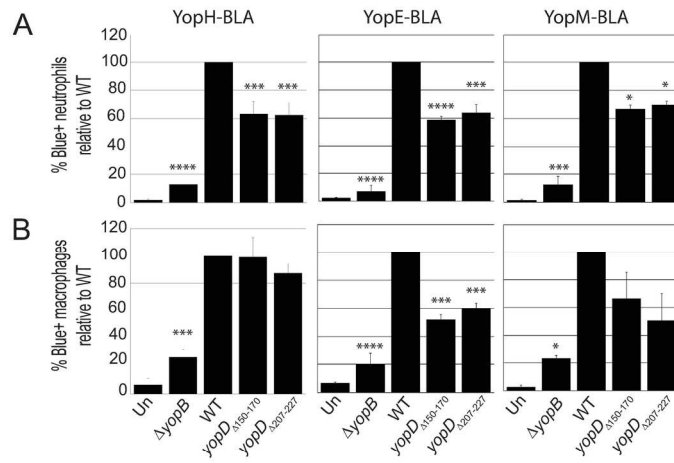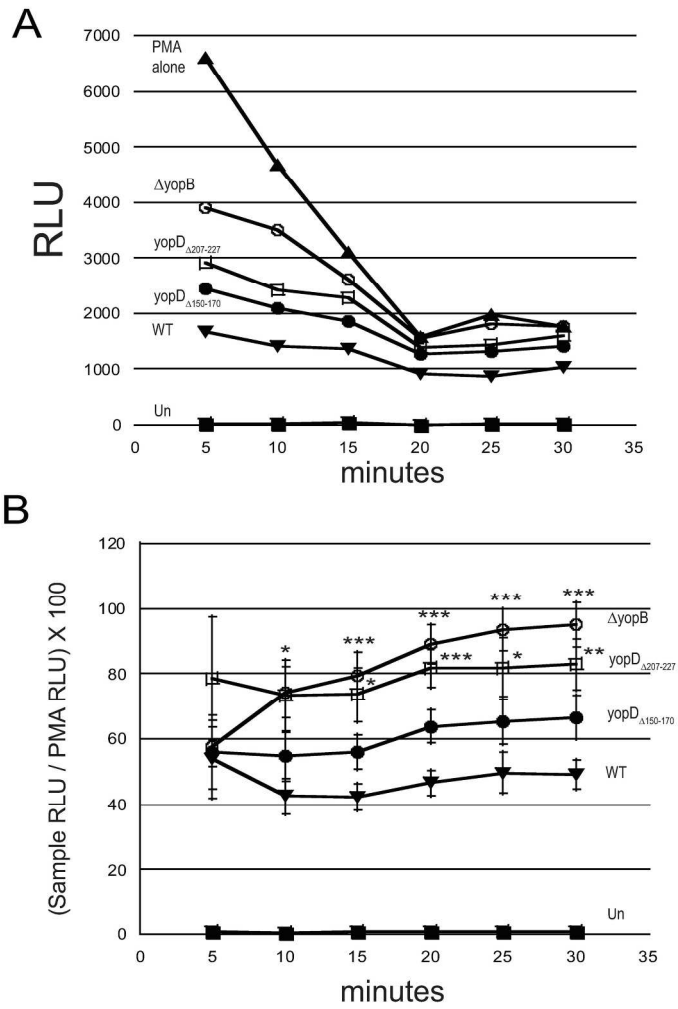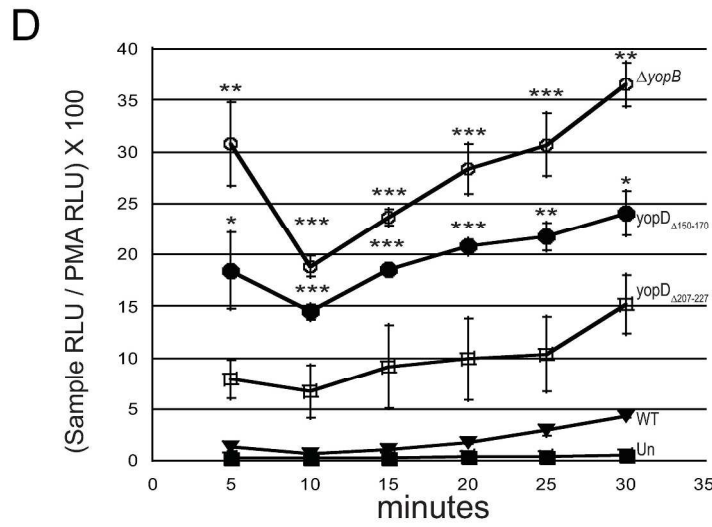

171x135mm (300 x 300 DPI)
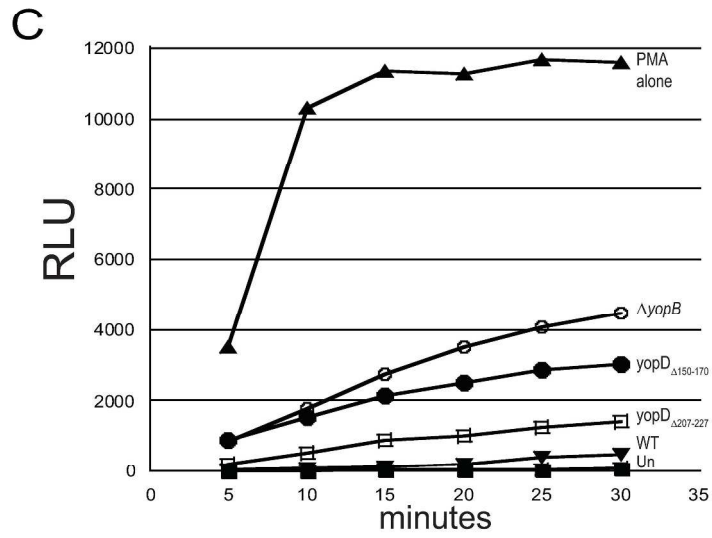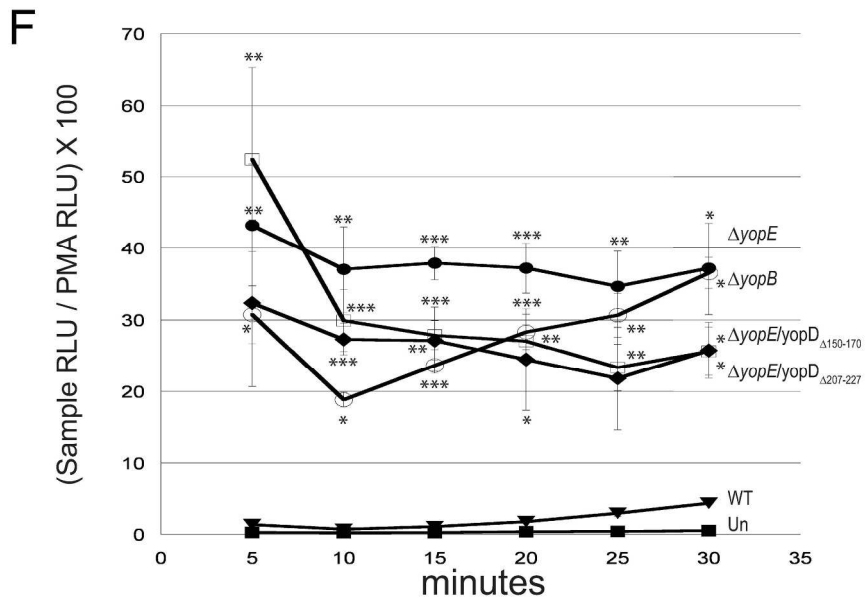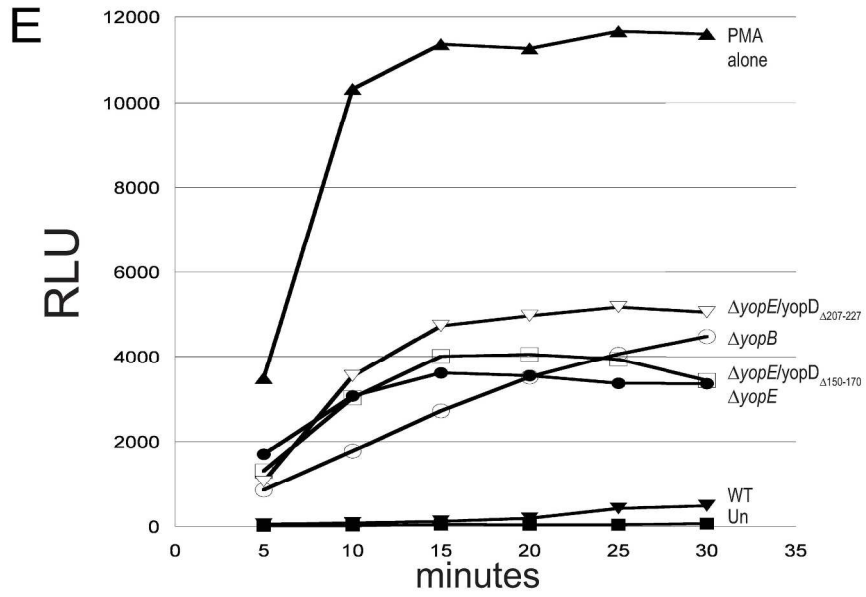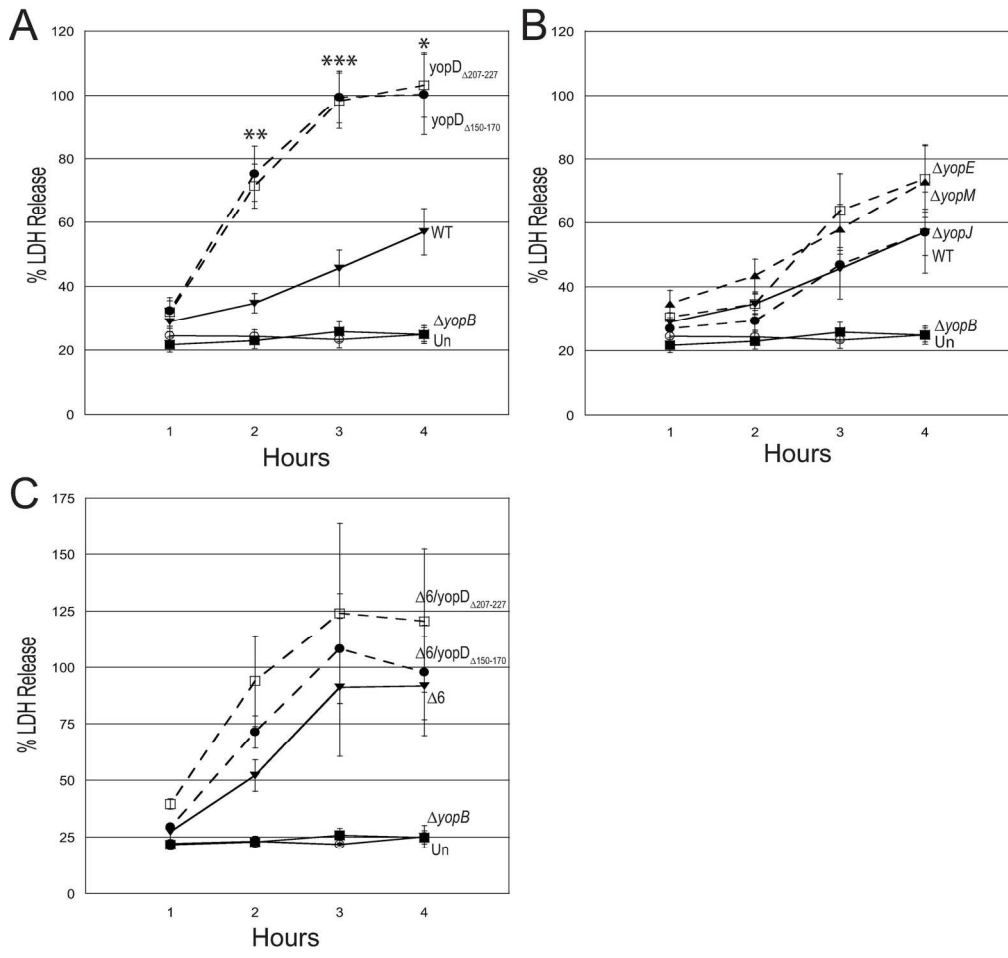
171x135mm (300 x 300 DPI)

221x230mm (300 x 300 DPI)

235x399mm (300 x 300 DPI)

213x287mm (300 x 300 DPI)

157x149mm (300 x 300 DPI)